九十一年度太空科技任務導向
委託研究計畫期末報告

中文計畫名稱：

Ka 頻段多點波束小型衛星通訊天線之研究

英文計畫名稱：

Development of A Ka-Band Multiple-Spot-Beams Antenna For Small-Satellite Communications

申請機構： 國立交通大學

執行單位： 電信工程系所

主 持 人： 鍾 世 忠 教授

共同主持人：張 志 揚 教授

日 期： 中 華 民 國 92 年 6 月 10 日

ABSTRACT

This project developed a new beam-steering millimeter-wave folded reflectarray antenna using printed-circuit planar reflectors. The folded reflectarray antenna consists of three parts: a main reflector, a sub-reflector, and a feed antenna. The main reflector contains hundreds of microstrip antennas used to produce twisted re-radiated fields and provide phase compensation for focusing. The sub-reflector parallel to the main reflector is made of a substrate printed with high-density metal grids, which are transparent to one polarization but would reflect the other polarization. The feed antenna is a microstrip patch antenna located on the main reflector. The position of this feed antenna is movable so as to steer the radiation-beam of the antenna. In addition, we developed a folded reflectarray antenna with three fixed-position feed antennas for beam switching capability. A fast beam switching can be realized by an electronic switch.

Introduction

For broadband wireless communications, MM-wave technology has moved toward a wide variety of practical uses, such as satellite communications, broadband wireless LAN, fixed wireless access, local to multi-points distribution service (LMDS), and short-haul personal communication networks (PCNs)[1]-[4]. Especially, the MM-wave systems exhibit the advantages of compactness, less weight, and high resolution, and are thus suitable for use in sensor radars such as Automotive collision avoidance radars [5]-[8], remote sensing satellites, SAR satellites, and security communications.

The purpose of this project is to develop a 38 GHz millimeter-wave antenna with three switching spot radiation beams. Each radiation beam has a beamwidth less than 5° and antenna gain about 25 dBi. The antenna is to be designed using the folded reflectarray type, containing a feed microstrip antenna, a main reflector for twisting and focusing, and a sub-reflector for polarization selection. This type of antenna has the advantages of low-profile configuration, compact structure, and easy to switch or steer the beams, which is thus suitable for small satellite and micro satellite communications.

The operation of this type of antennas is similar in concept to a conventional parabolic reflector antenna. But it combines the advantages of reflectors and phased arrays. For these reasons, we design the antennas with high gain, low side-lobe levels, and low loss, in the following configuration.

1. The folded reflectarray, like the conventional Cassegrain or Gregorian reflector antennas, reduces the large size of the general reflector antenna caused by the long focal length.

2. The omission of the supporting arm for the feed antenna also avoids the blocking effect and reduces the required length, and thus the propagation loss, of the feed line.

3. As compared to a phased array, the reflectarray needs no complex feed network. The field from the feed antenna is spatially fed to the individual elements in the flat array, without suffering from high propagation loss in a complex feed network, especially at MM-wave frequencies [10]-[14].

4. When the position of the feed antenna is shifted, the radiation beam direction of the folded reflectarray will change. The tunable radiation beam can be easily done.

2. Status

The design, analysis, and measurement of the element of the main reflector, feed antenna, and sub-reflector have been finished respectively. The whole reflectarray antenna and a switchable multi-beam antenna are also developed. These antennas have low profile configuration and suitable for mechanical beam scanning or electronic beam switching, and work very well in practice.

3. Theory and Design

3.1 Total structure view:

Reflectarrays, which were first presented by Berry in 1963 [15], combine the advantages of reflectors and phased arrays. And other relative designs are developed by many people [16]-[22]. The folded reflectarray antenna contains a main reflector, a sub-reflector, and a feed antenna, as illustrated in Fig. 3.1-1. The main reflector is separated from the sub-reflector with a depth of H. In this project, the depth H was fixed as 23 *mm*, or 2.95 λ (wavelength) at the designed frequency of 38.5 GHz. The main reflector is a reflectarray that consists of hundreds of square patch antennas distributed in a circular substrate region with diameter D. The sub-reflector is a low-loss substrate printed with high-density metal grids. The feed antenna is a probe-fed rectangular patch antenna located on the same substrate as the main reflector. Each square patch element on the main reflector is placed with 45° tilted to the feed antenna. The flow chart of design, implementation and measurement is illustrated in Fig. 3.1-2.

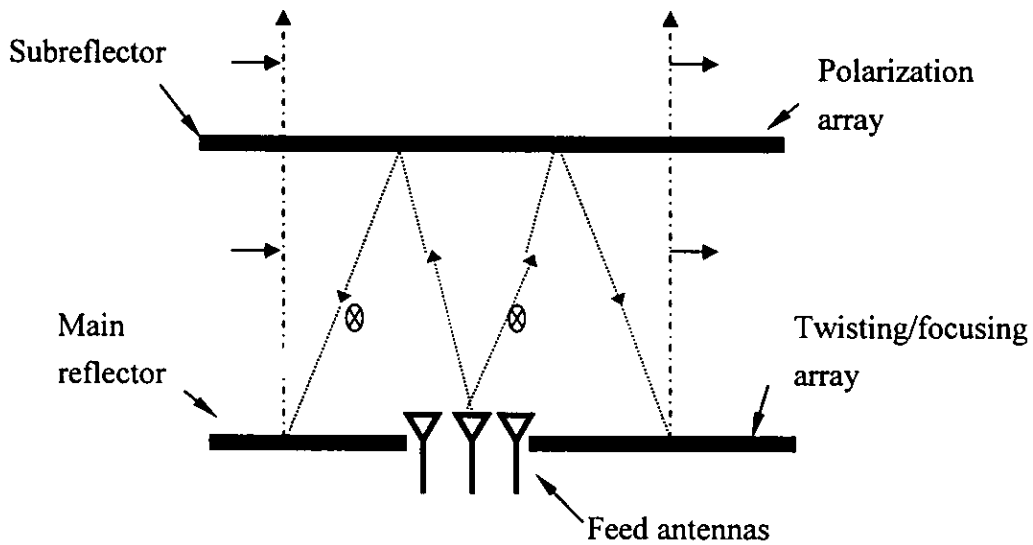

Fig 3.1-1 Configuration of the reflectarray antenna

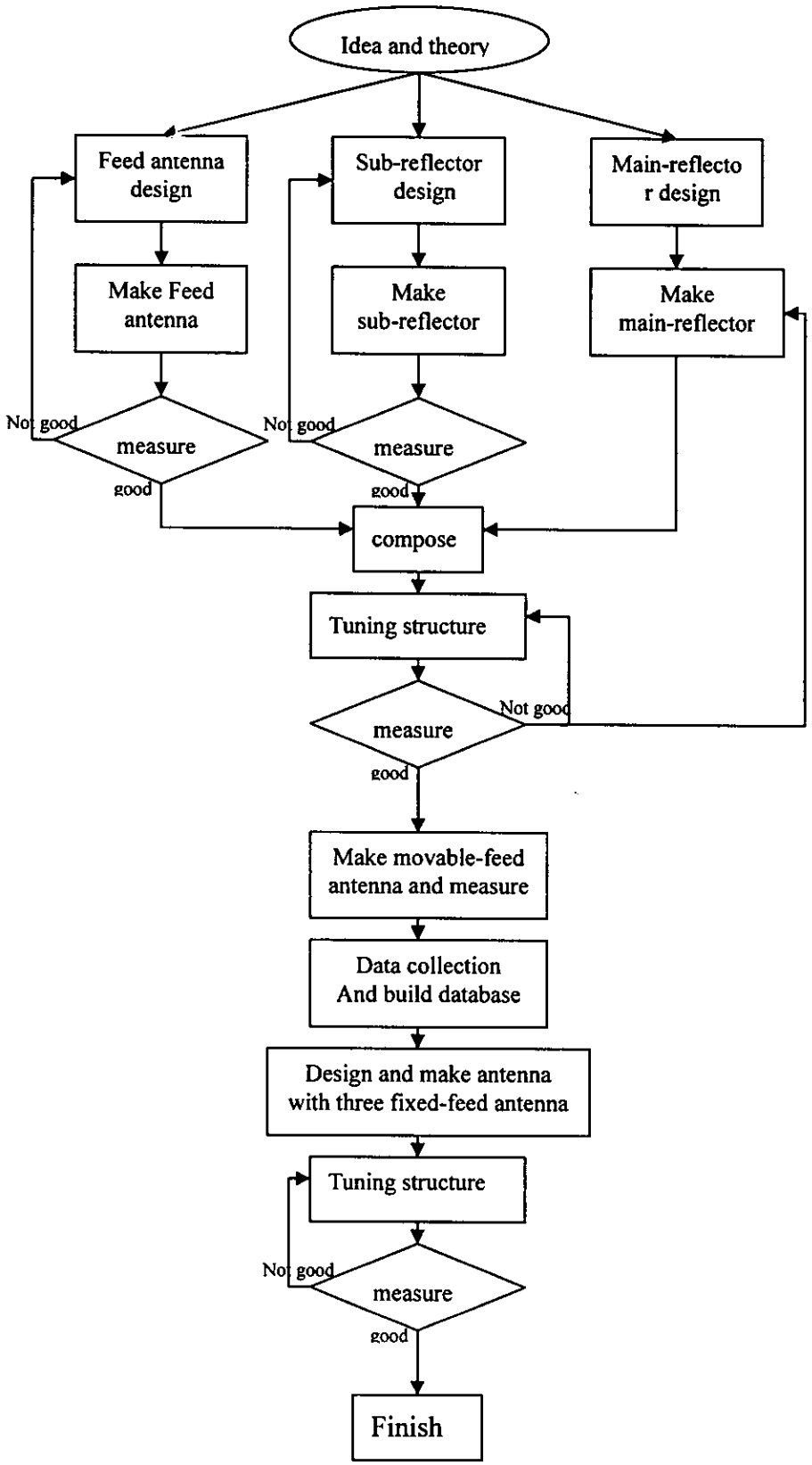

Fig 3.1-2 The flowchart of design, implementation and measurement

3.2 Design of each part

To complete the whole structure, each part of the folded reflectarray antenna should be properly designed to achieve its specific effect. The details are described as follows.

Feed antenna:

The feed antenna is a probe-fed rectangular patch antenna with the length of 2.3 *mm* and the width of 2.4 *mm*, which is located on the same substrate as the main reflector.

Sub-reflector:

The feed antenna illuminates a y-directed electric field toward the sub-reflector that is composed of y-directed close-spaced metal lines. Since the polarization of incident fields parallel to the metal lines, it will be reflected by the sub-reflector and received by the square patch elements on the main reflector. By the image principle, the reflected wave can be regarded as generated by an image feed antenna located at $z = 2H$. After many times of the experiments, both the width and the spacing of the metal strips are determined to be 0.1 mm, as shown in Fig. 3.2-2. The sub-reflector functions as a polarization selector. It reflects the fields of one polarization radiated from the feed, and is transparent to the re-radiated fields from the main reflector.

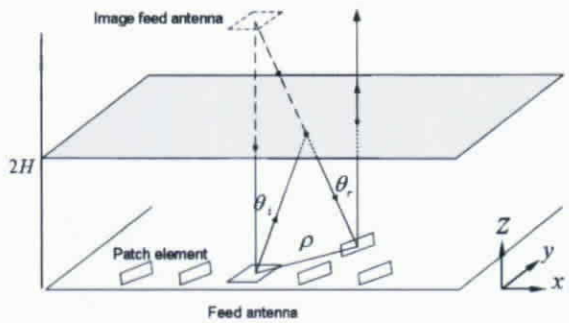

Fig 3.2-1 The coordinates of the reflectarray antenna

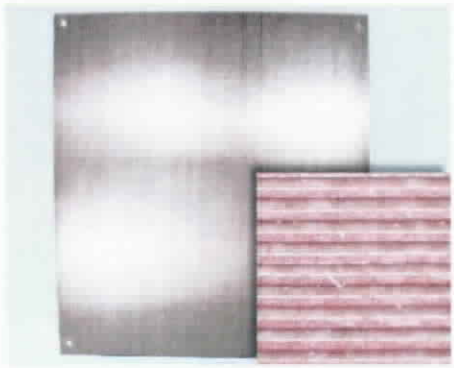

Fig 3.2-2 Picture of the sub-reflector

The element of the reflectarray:

Fig 3.2-3 shows the schematic diagram of the elements on the main reflector. According to the design principle, the elements on the main reflector have the functions of twisting the fields and focusing. The open microstrip stubs connected to each square patch antenna would twist the fields and generate x-directed re-radiation fields, as shown in 3.2-4. Also, the phase delay at each square patch will be compensated by the open stubs. Therefore, the antennas on the main reflector form an array excited with uniform phases and tapered amplitudes distribution. Open stub length of each element is determined according to its location. Properly arrange the elements and compute the corresponding length of open stub, we can generate a narrow radiation beam at the broadside direction. Note that, since the re-radiated field from the array is perpendicular to the metal lines, it could penetrate through the sub-reflector with negligible loss. The picture of the elements on the main reflector is shown in Fig. 3.2-5.

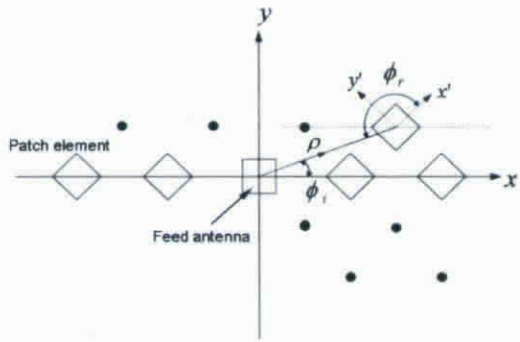

Fig 3.2-3 Schematic diagram of the elements on the main reflector

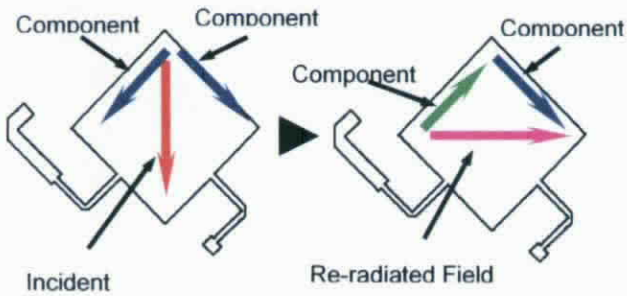

Fig 3.2-4 The polarization of re-radiated field is perpendicular to that of the incident field

Fig 3.2-5 Picture of elements on the main reflector

The main reflector for fixed radiation beam:

As described in the previous sections, the main reflector is an array of patch antennas. The elements on the substrate are of the same sizes but with different length of the open stubs. Depending on the distance from the feed to the element, the lengths of the open stubs of each element are determined. The actual layout of the main reflector is shown in Fig 3.2-6. Note that, the feed patch is located at the center. Fig 3.2-7 is the picture of top view and bottom view of the finished folded reflectarray antenna. The measurement results are shown in the later.

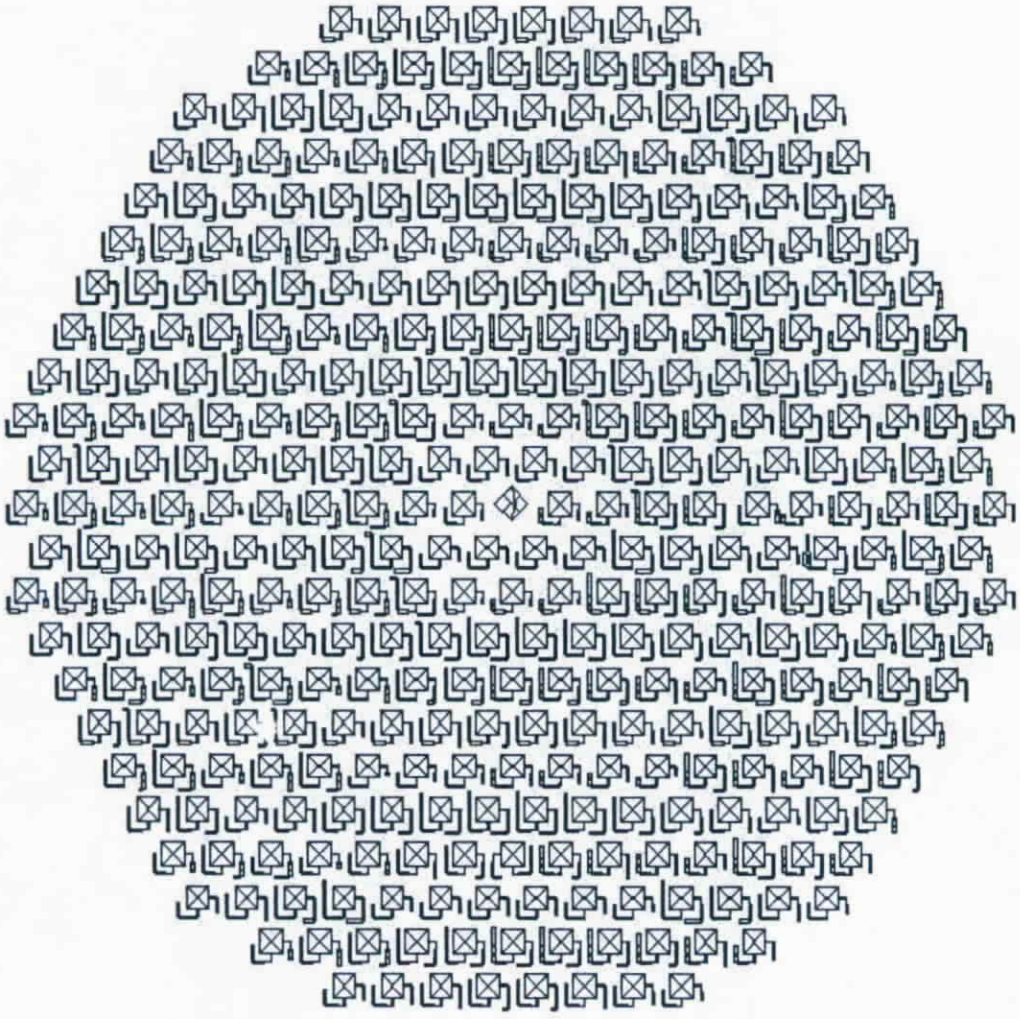

Fig 3.2-6 Layout of the main reflectarray

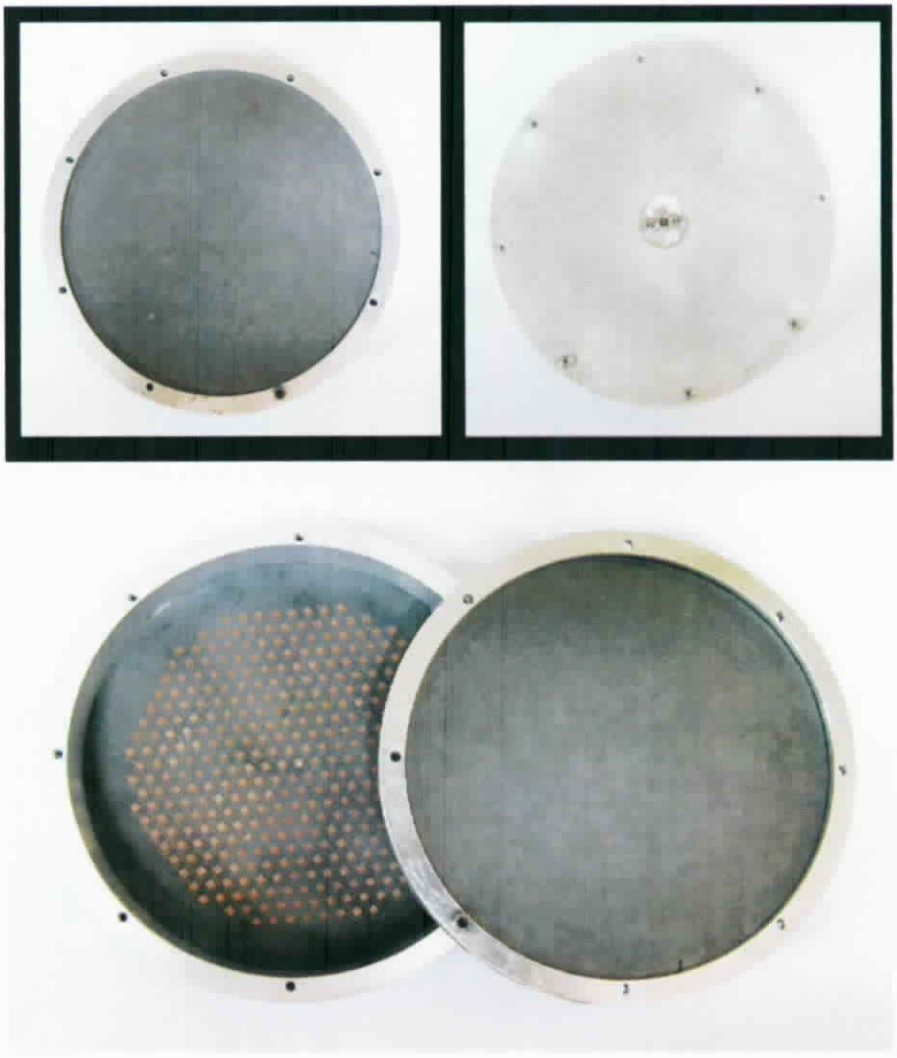

Fig 3.2-7 Top view and bottom view of the finished folded reflectarray antenna

<u>The structure for steering radiation beam with movable feed antenna:</u>

When the position of the feed antenna is shifted, the radiation beam direction of the folded reflectarray will also change. As shown in Fig. 3.2-8, the movable feed antenna shifts the distance d, the path length from the shifted feed antenna to the mth square patch changes from the original value r_m to a new value r_m'. The path length variation has negligible influence on the excitation power, but would result in a change of the excitation phase equal to $k_0\Delta r_m$, $\Delta r_m = r_m - r_m'$. The resultant antenna gain pattern thus has the same formula as with a new normalized array factor that we will illustrate in the next part.

For collecting the data of the relation between the feed antenna movement and the beam direction, we designed a movable platform for the feed antenna to change the position. Fig. 3.2-8 shows the structure of the folded antenna with the movable feed antenna. The aperture diameter D of the folded reflectarray is set as 100 *mm* and height H is 23 *mm*. The feed antenna moves along the x direction from d = -4 *mm* to +4 *mm*. When d = 0 *mm*, the radiation beam points to the broadside direction. Fig. 3.2-9 shows the equivalent structure of that antenna with the shifted feed antenna and its corresponding beam direction. By measurement, it is found that as d changes from –4 *mm* to +4 *mm*, the main beam directs from +3.8° to –3.8°, and the corresponding first side lobe moves from the left hand side of the main beam to the right hand side. The beam steering rate is about 1° per 1 *mm* movement. It is also noticed that the side lobe level rises with the increase of the feed position deviation.

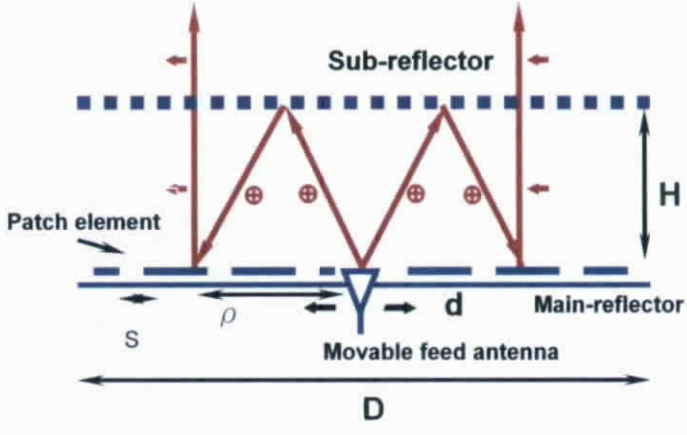

Fig 3.2-8 Structure of the folded antenna with the movable feed antenna

Fig 3.2-10 shows the picture of the movable feed folded reflectarray antenna. The movable feed antenna is located in the center of the main-reflector. Relation between the beam direction and the position of the feed antenna is measured, and the measurement results are provided in the later.

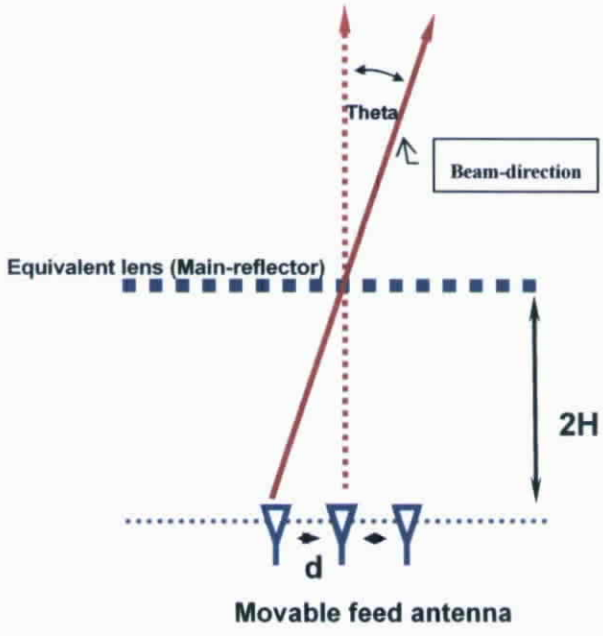

Fig 3.2-9 The relationship of feed position and beam direction

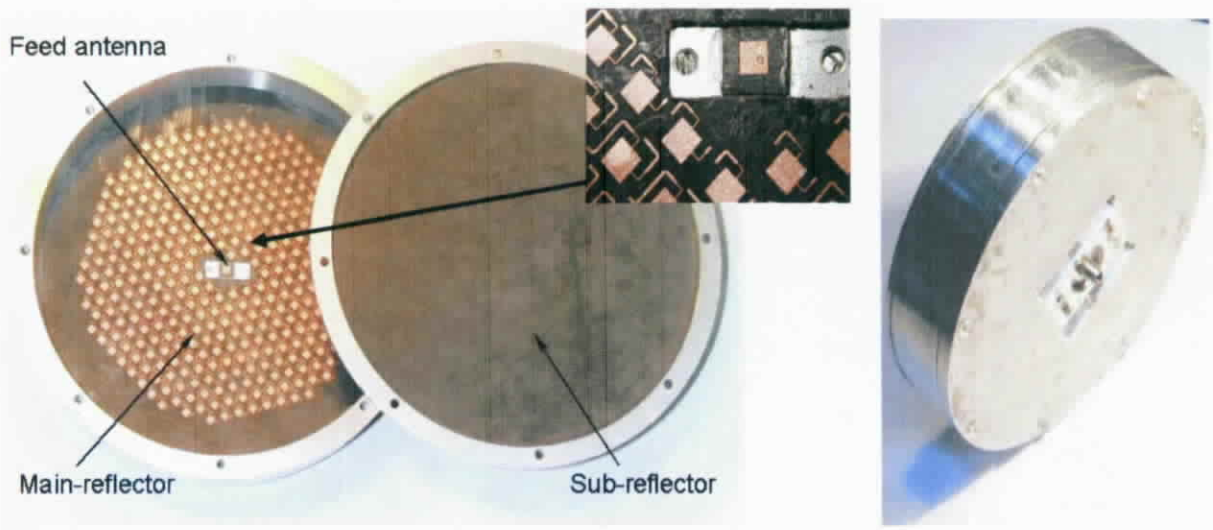

Fig3.2-10 Picture of the folded reflectarray antenna with a movable feed

Switched-beam antenna structure with three fixed feeds:

In order to have a faster beam-switching capability, the antenna is designed to have multi-fixed feeds. The multi-direction beam can be realized by exciting different feed instead of moving the feed. The electronic switch mechanism can be used here. To design this structure, the choice of the feed position is one of the important parameters. According to the measurement result of movable feed antenna, the relation between the feed position and beam direction is obtained. Therefore, we can determine the position by choosing the beam direction we are interested and looking up the measurement data. Here we wish to have the wider beam switching range; so the position of *+/- 12.5mm* is chose as the feed position. We increase the diameter of main-reflector for more efficiency. Fig 3.2-7 is the picture of top view and bottom view of the antenna with three fixed feeds.

Fig 3.2-11 The top and bottom view of the antenna

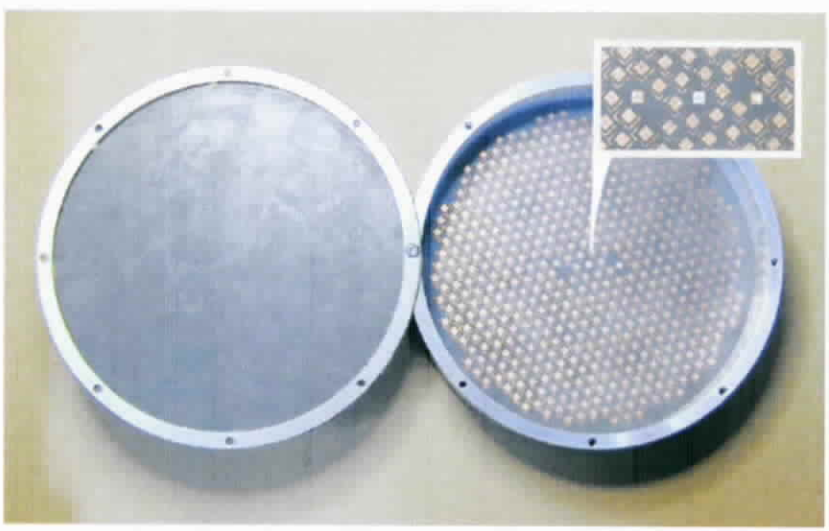

Fig 3.2-12The cross-sectional view of the antenna

4. Simulation and analysis:

Patch antenna's pattern:

The normalized far-field components of a rectangular patch antenna fed in the y direction can be expressed as follows [20]:

$$E_\theta = \sin\phi \; h(\theta,\phi) \tag{1a}$$

$$E_\phi = \cos\theta \; \cos\phi \; h(\theta,\phi) \tag{1a}$$

$$h(\theta,\phi) = \frac{\sin\left[\frac{k_0 W}{2}\sin\theta\cos\phi\right]}{\frac{k_0 W}{2}\sin\theta\cos\phi}\cos\left(\frac{k_0 L}{2}\sin\theta\cos\phi\right) \tag{2}$$

where k_0 is the free-space wavenumber. L and W are the length and width of the patch, respectively. Note that the x-directed electric field is zero in the above formulas. Fig 4-1 is the simulated pattern of a patch antenna.

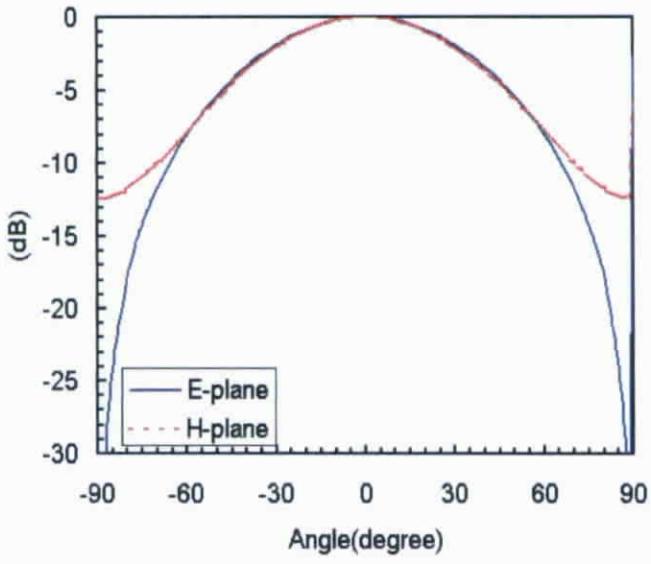

Fig 4-1 Simulated pattern of a patch antenna

Power distribution:

The Friis transmission formula is used for analysis:

$$P_r = P_t \frac{G_t G_r \lambda^2}{(4\pi r)^2} \tag{3}$$

where P_r and P_t are respectively the received and the transmitted powers of a receiving antenna (with gain of G_r) and a transmitting antenna (with gain of G_t) separated at a distance of r. Let G_f and G_{sq} be the broadside antenna gains of the feed antenna and the square patch antenna, respectively. The antenna gains at the direction of (θ, ϕ) are thus correspondingly equal to $G_f\, g_f(\theta, \phi)$ and $G_{sq}\, g_{sq}(\theta, \phi)$, with $g_i(\theta, \phi)$, $i = f$ or sq, being the normalized power pattern of the patch antennas:

$$g_i(\theta,\phi) = E_\theta^{\,2}(\theta,\phi) + E_\phi^{\,2}(\theta,\phi) \tag{4}$$

Now refer to Fig. 3.2-3. Let the input power fed to the feed antenna be P_i. The power P_m received by the mth square patch can be calculated from (1) and written as

$$P_m = P_i \frac{G_f g_f(\theta_i,\phi_i) G_{sq} g_{sq}(\theta_i,\phi_i + 3\pi/4)\lambda^2}{(4\pi r_m)^2} \tag{5}$$

or

$$P_m = P_i G_f G_{sq} C_m \tag{6}$$

with C_m defined as

$$C_m = \frac{g_f(\theta_i,\phi_i)\, g_{sq}(\theta_i,\phi_i + 3\pi/4)\lambda^2}{(4\pi r_m)^2} \tag{7}$$

Here r_m is the distance between the mth square patch and the image feed antenna,

$$r_m = \sqrt{(2H)^2 + \rho_m^{\,2}} \tag{8}$$

with ρ_m being the distance between the square patch and the feed antenna. Noticed that for an illuminating angle of (θ_i, ϕ_i) from the feed antenna, the wave receiving angle for the mth square patch is $(\theta_i, \phi_i + 3\pi/4)$.

As assumed above, the received power by each square patch antenna is fed back to the same antenna and re-radiated out. It is seen from (5) that, this excitation power reduces as the distance ρ_m between the square patch and the feed antenna increases. Fig. 4-2 shows the calculated excitation power distribution as function of ρ_m.

The total radiation power P_{rad} at an angle of (θ, ϕ) from the in-phase excited array equals the element antenna pattern $G_{sq}\, g_{sq}(\theta,\phi)$ times the array factor pattern $F^2(\theta, \phi)$, that is,

$$P_{rad}(\theta,\phi) = G_{sq} g_{sq}(\theta,\phi) \cdot F^2(\theta,\phi) \tag{9}$$

where

$$F^2(\theta,\phi) = \left| \sum_m \sqrt{P_m} \cdot e^{jk_0(x_m \sin\theta\cos\phi + y_m \sin\theta\sin\phi)} \right|^2 \tag{10}$$

with (x_m, y_m) being the global coordinates of the mth square patch antenna. By casting (6) into (10), and using (9), the total antenna gain pattern G_{total} of the folded reflectarray antenna can be derived as

$$\begin{aligned} G_{total}(\theta,\phi) &= P_{rad} / P_i \\ &= G_f G_{sq}^2 \cdot f^2(\theta,\phi) \end{aligned} \tag{11}$$

with the normalized array factor defined as

$$f^2(\theta,\phi) = g_{sq}(\theta,\phi) \left| \sum_m \sqrt{C_m} \cdot e^{jk_0(x_m \sin\theta\cos\phi + y_m \sin\theta\sin\phi)} \right|^2 \tag{12}$$

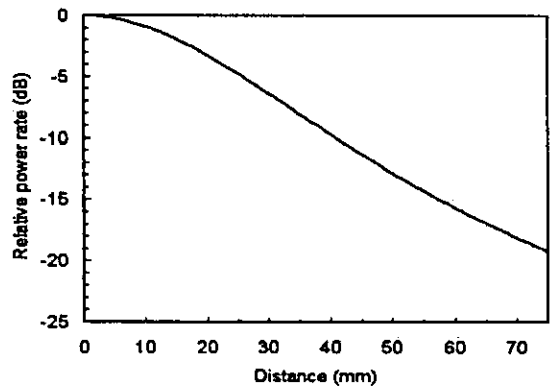

Fig 4-2 Relative power with respect to the distance from the feed

When the position of the feed antenna is shifted, the radiation beam direction of the folded reflectarray will change. To simulate this effect, it is noticed from Fig. 3.2-3 that, the image feed antenna shifts the same amount as the feed antenna does. The path length from the image feed antenna to the mth square patch changes from the original value r_m to a new value r_m'. The path length variation would result in a change of the excitation phase equal to $k_0\Delta r_m$, $\Delta r_m = r_m - r_m'$. The resultant antenna gain pattern thus has the same formula as (12) with a new normalized array factor of

$$f^2(\theta,\phi) = g_{sq}(\theta,\phi) \left| \sum_m \sqrt{C_m} \cdot e^{jk_0(x_m \sin\theta\cos\phi + y_m \sin\theta\sin\phi + \Delta r_m)} \right|^2 \tag{13}$$

Aperture efficiency:

The efficiency of a reflectarray is usually not as high as compared to a conventional reflector antenna of the same size. This is because that only part of the area (that is, the area covered with printed antennas) illuminated by the incident wave generates effective radiation field. As reported in relative literatures, the typical values of the reflectarray's aperture efficiency range from 10% to 30%. Fig. 4-3 shows the calculated aperture efficiency, as a function of the aperture's diameter D, of the present folded reflectarray antenna. As the antenna size increases, the efficiency first increases due to the rapid growth of the antenna gain, and then decreases because of the saturation of the gain. This is because that the excitation power of the square patch antenna decays rapidly as the patch moves far away from the feed antenna. For example, as seen from Fig. 4-2, the excitation powers of the patches located outside a circular region of radius 50 *mm* are below –13 dB. The calculated efficiency is higher than 15% when the diameter is located between 80 *mm* to 140 *mm*. A maximum efficiency of 16.1% can be achieved as D equal to about 100 *mm*.

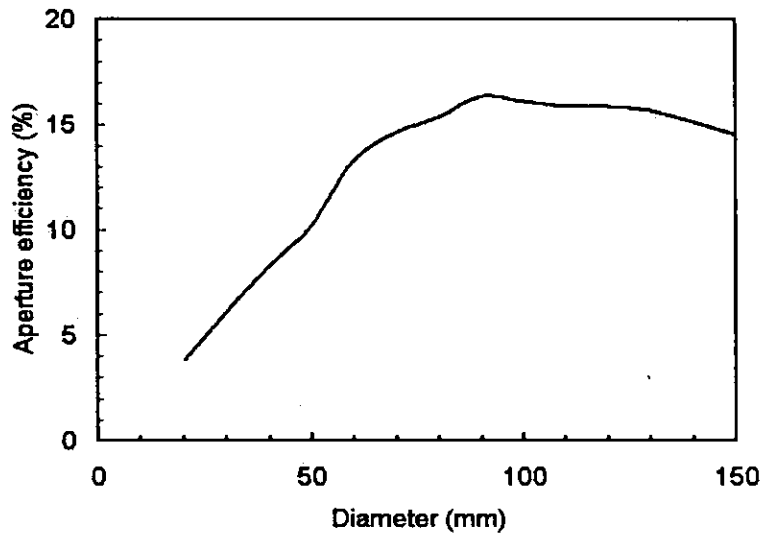

Fig 4-3 aperture efficiency

Another aperture efficiency of the reflectarray antenna was defined by David M. Pozar [10], where, instead of using the whole aperture size, the total area of the printed antennas on the reflectarray was used to calculate the aperture's maximum directivity. Resultant aperture efficiencies are between 20% to 65% for millimeter-wave reflectarrays were reported [10]. Under this definition, the corresponding aperture efficiency for the present folded reflectarray with $D = 100$ *mm* is calculated to be 60%. Then the choice of the diameter D for the antenna can be depended by the aperture efficiency simulation.

5.Measurement:

The feed antenna:

The return loss of the feed Antenna is (S_{11}:-15.5dB , Bandwidth:3.1GHz, 8%)

Feed antenna pattern(gain:6.5dBi, 3dB-beamwidth: 93°)

Fig 5-1 Picture of the feed antenna

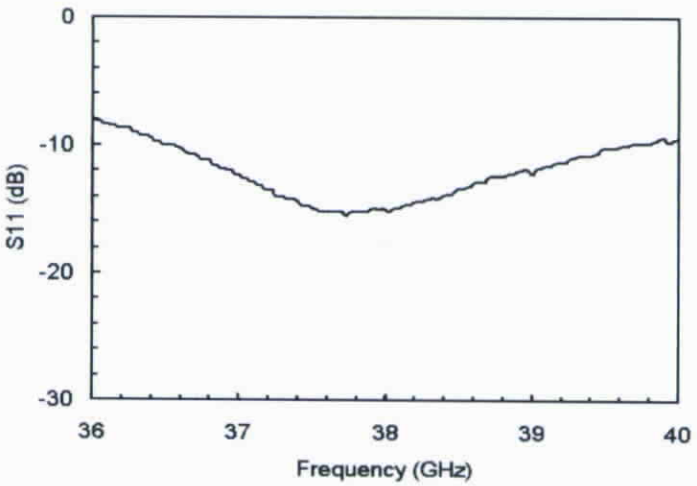

Fig 5-2 The measured return losses of the feed for various frequency

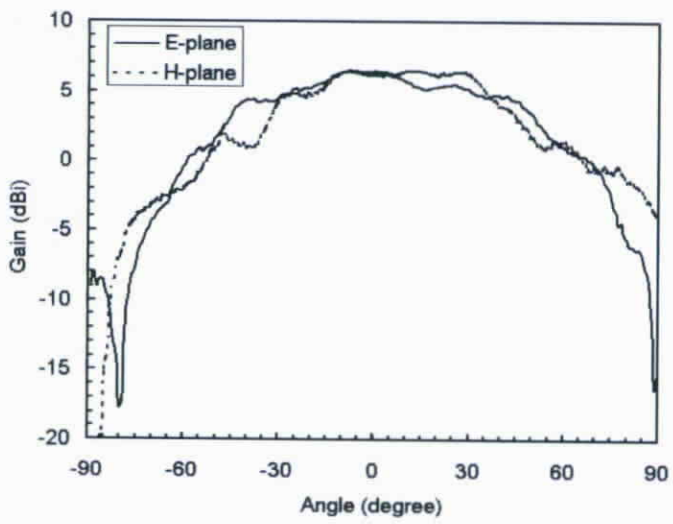

Fig 5-3 The measured gain of the feed antenna

The elements on the main reflector:

S-parameter of the patch element of the main reflector

(S11:-34.5dB, S21<-19dB, BW: 2GHz)

Patch element pattern of the main reflector

(gain: 5.6dBi, 3dB-beamwidth: 88°)

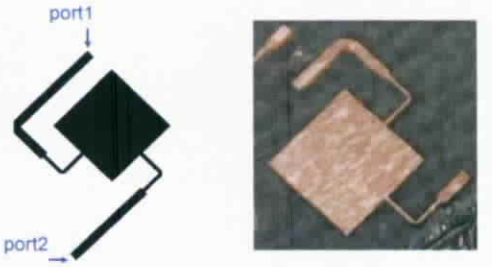

Fig 5-4 picture of the element

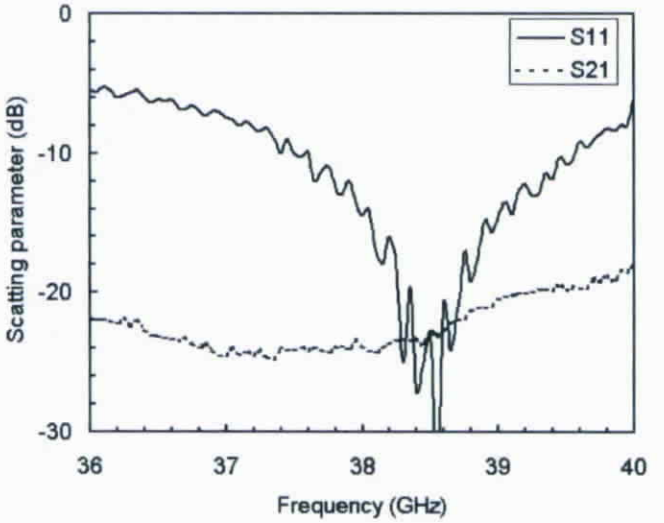

Fig 5-5 measured S-parameter of the

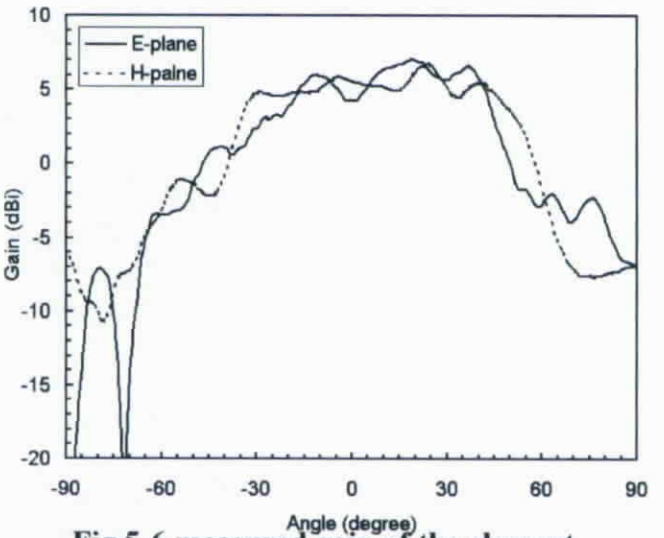

Fig 5-6 measured gain of the element

The sub-reflector:

To have a better understanding, several investigations have been done on the sub-reflector. The table below is the measurement of the sub-reflector, for various metal grid spacings, with grid lines parallel or perpendicular to the transmitting waves. The result shows the isolation of the polarization is very well. The sub-reflector can suppress the orthogonally polarized waves up to 34db. The insertion loss in the substrate Duroid 5870 is quite small. The polarization isolation of the sub-reflector also provides good polarization effect. Though the high cross polarization is the nature of the probe-fed patch antenna. Through the sub-reflector, the cross polarization will be reduced significantly.

Transmission wave	**Received Power**	**Loss in Substrate (Duroid 5870)**
↑ Output Power :8dBm	**↑ air: –14.17dBm**	
	→ air: –32.17dBm	
	↑ horizontal metal grid:-14.33dBm	**0.16dB**
	↑ vertical metal grid:-48.5dbm	**34.17dB**
	→horizontal metal grid:-49.5dBm	**17.33dB**
	→vertical metal grid:-34.67dBm	**2.5dB**
↑ :vertical polarization EM-wave → : horizontal polarization EM-wave The distance between transmitter and receiver is 230mm		

The measured return loss of the folded reflectarray antenna with a movable feed:

Apart from the single feed patch antenna, the measurement of the complete folded reflectarray antenna is taken. The moving mechanism of the feed antenna is shown as Fig 5-7.

When measuring the single patch antenna, the waves radiate without obstacle. As for the complete antenna, the feed antenna is on the center of the main reflector which is enclosed by a housing. Therefore, when waves radiate from the feed, the main-reflector, sub-reflector and the housing have effects on the radiation property and S-parameters. As shown in Fig 5-8, the return loss of the complete antenna is good in the frequency band interesting. The return loss S_{11} at 38.5 GHz -16dB.

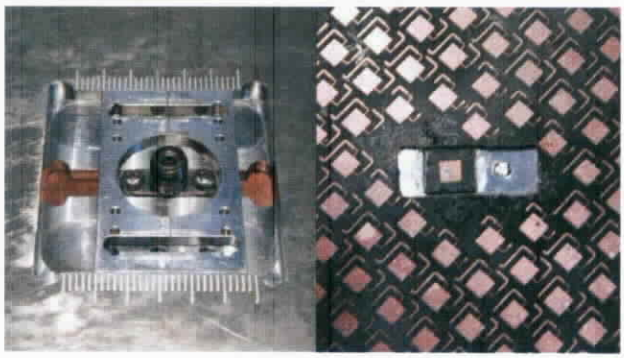

Fig 5-7 The moving mechanism of the feed antenna

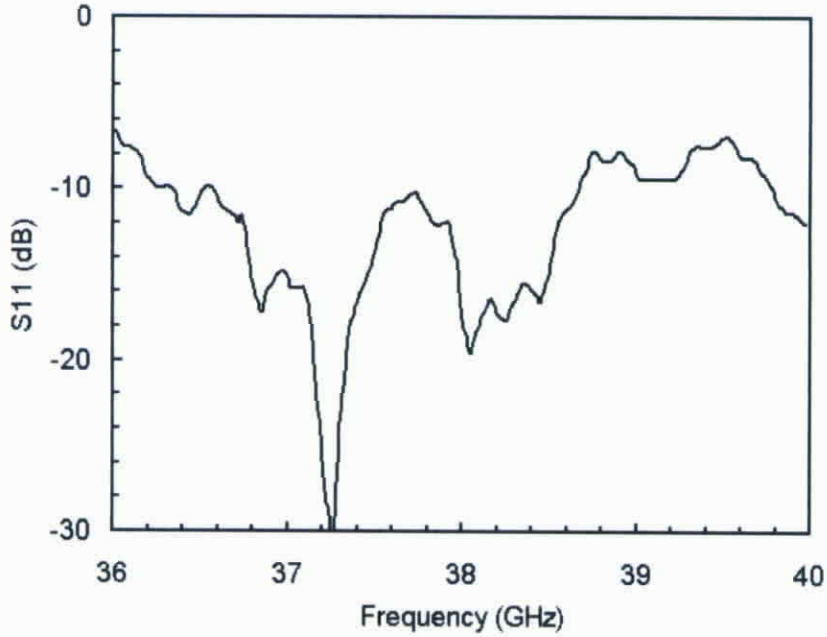

Fig 5-8 The return loss of the complete antenna

The measured pattern of the folded reflectarray antenna with a movable feed:

The antenna we design is for narrow beam application. Fig. 5-9 and 5-10 show the E-plane and H-plane pattern of the folded reflectarray antenna with a movable feed respectively. The 3-dB beam-width in E-plane is *5.6 degree*. Note that, the cross-polarization is very small.

The E-plane pattern:

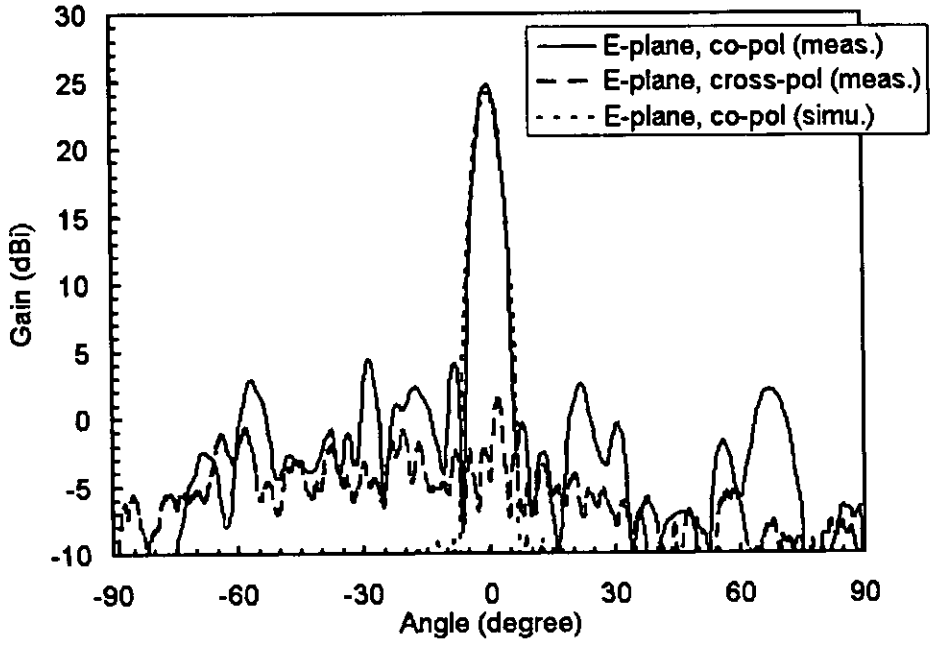

Fig. 5-9 E-plane pattern of the complete antenna

The H-plane pattern:

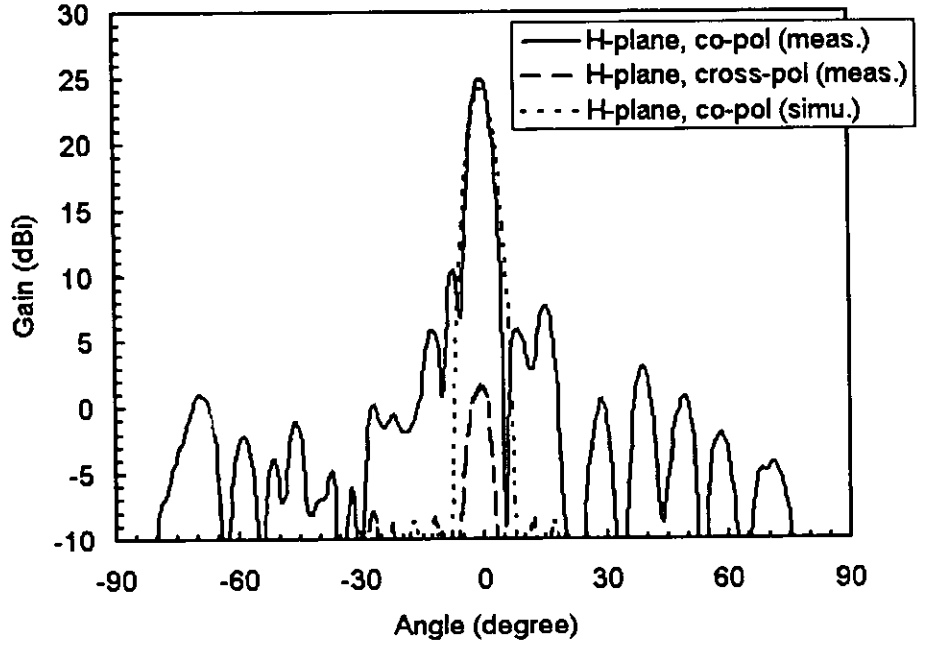

Fig. 5-10 H-plane pattern of the complete antenna

The E-plane patterns for different feed positions in 38.5GHz:

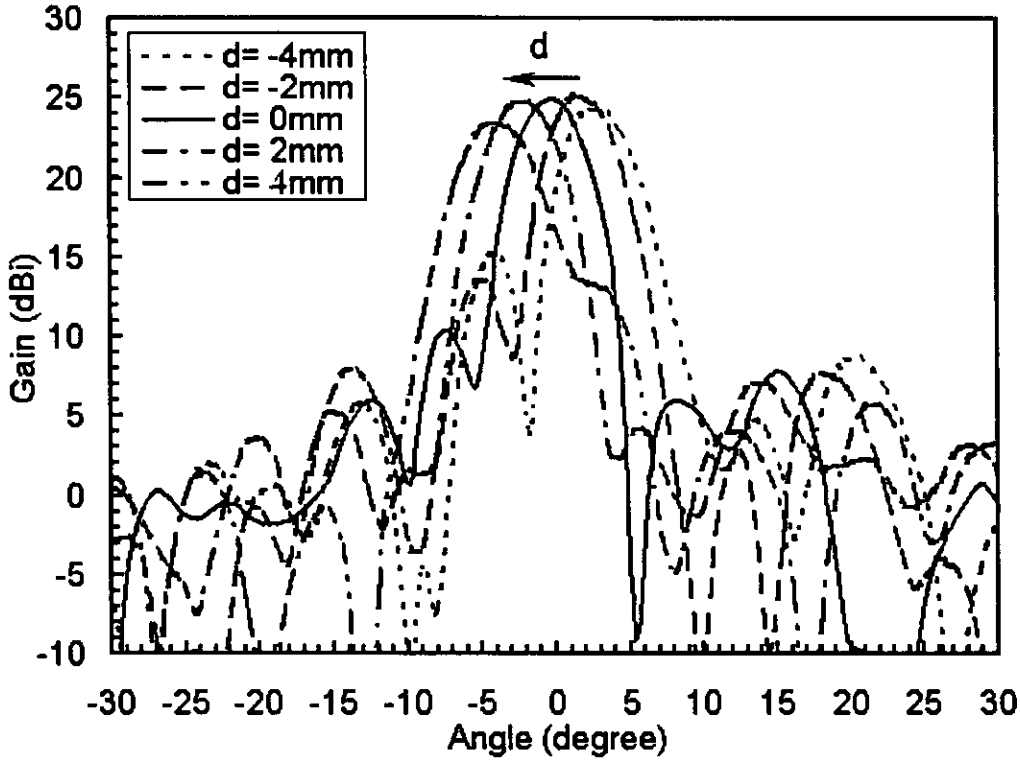

Fig. 5-11 E-plane patterns for different feed positions

The E-plane patterns for different feed positions displaced from the center of main reflector are measured and shown in Fig 5-11. As the figure shows, the beam direction is changed with the moving of the feed. The main beam direction for various displacement of the feed is shown in Fig. 5-12. It is found that the antenna gain is slightly decreased with the displacement. This is because the fields re-radiated from the patch elements on the main reflector are not completely in-phase in the main beam direction. However, the performance is still good.

The antenna gain with respect to the feed position is illustrated in the Fig 5-13. It is obviously that the gain is reduced when the feed is far from the center point. The longer distance, the lower gain. There is a trade off between the scanning range and the antenna gain. When designing a beam-steering reflectarray antenna, this is a important consideration.

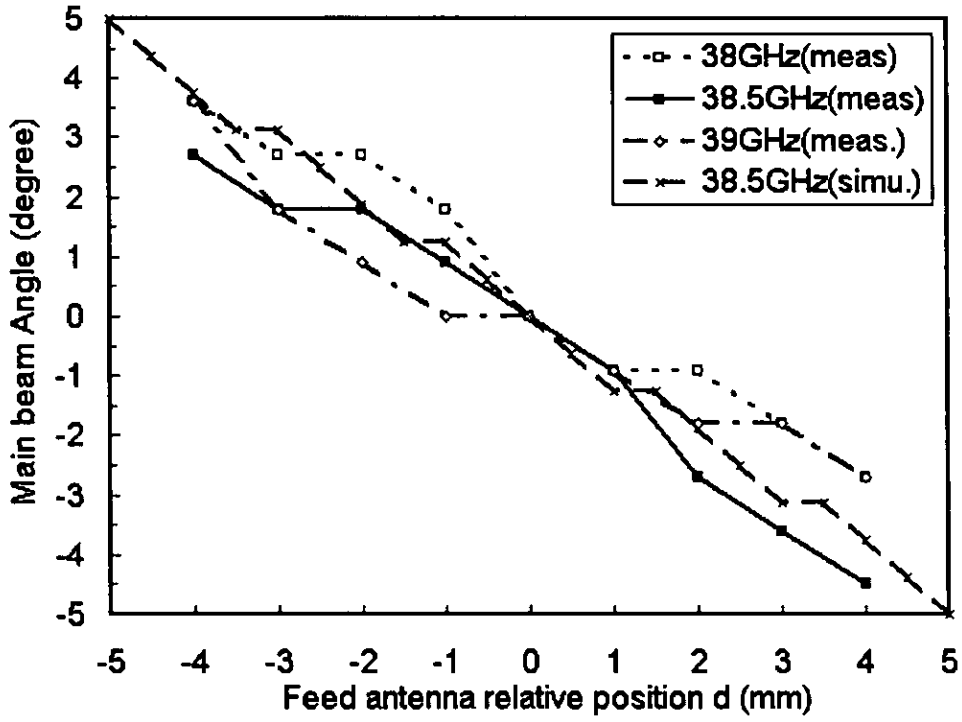

Fig. 5-12 The main beam direction for various displacement of the feed

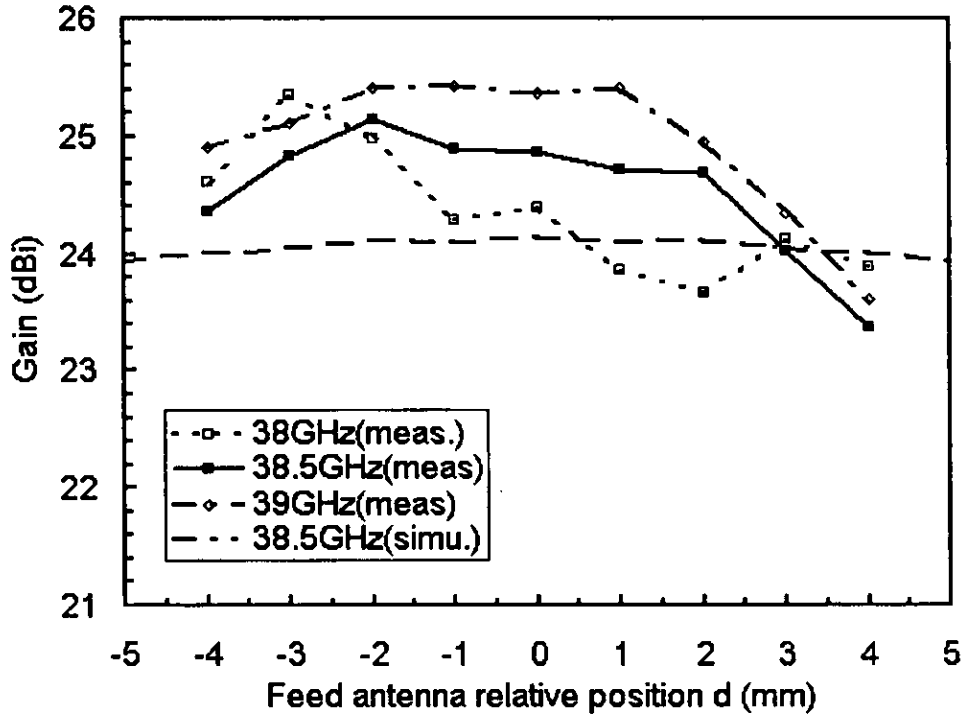

Fig. 5-13 The antenna gain with respect to the feed position

The patterns of the finished folded reflectarray antenna with three fixed-feeds:

The final measurement is the pattern of the finished folded reflectarray antenna with three fixed-position feeds. In this antenna, the diameter of the main reflector is increased for a better efficiency. The measured result is plotted in Fig5-14. Obviously the gain is better than previous ones. The antenna gain of the off-center fed pattern is lower than the one fed by center feed. The center-fed gain is *27dBi*, and the gain of the off-center fed pattern is *22.6dBi*. The beamwidths of three patterns are quite close, but the off-center fed beam is a little wider. For the case of the feed located at *d=12.5mm* from the center, the main beam direction is about *15 degrees*. That is, the total steerable rotation angle is about 30 *degrees*. This range is wide enough for many applications, such as Automotive Collision Avoidance Radars, LMDS, remote sensing satellites and communication satellites.

The E-plane pattern of the finished antenna with the three different-position feed:

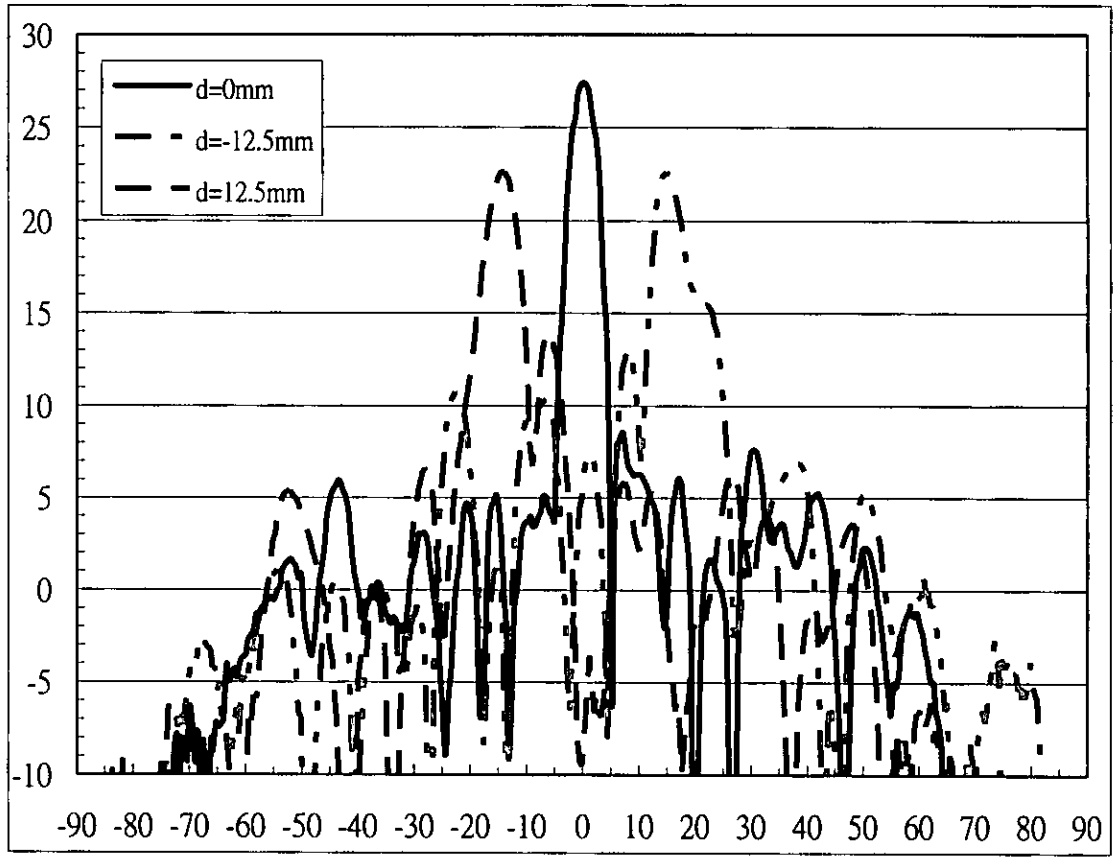

Fig 5-14 the three switch able beam pattern

Reference:

[1]A. Nordbotten, "LMDS System and Their Application, " *IEEE communication Magazine,* vol. 38, Issue 6, June 2000, pp. 150-154

[2]J. Shaker and M. Cuhaci "Planar Reflector for LMCS applications" *Electronics Letters 21st*, vol. 35, no. 2, January 1999, pp. 103-104

[3]G. Wu, M. Inoue, H. Murakami, and Y. Hase "156Mbps Ultrahigh-Speed Wireless LAN Prototype in The 38GHz Band" GLOBECOM '01. IEEE, vol. 6, 2001 pp. 3573-3578.

[4]H. H. Meinel, "The Market for Short-haul-of-sight Millimeterwave Transmission Links" *IEEE MTT-S Digest*, 1996, pp. 487-489.

[5]E. Hayman, Y. Kalatizadeh, R. Pearson, M. W. Shelley, and J. Vazquez "Novel Reflector Antenna Design for ACC Applications" *Antennas for Automotives, IEEE Colloquium on*, 2000, pp. 3/1-3/6

[6]M. E. Russell, A. Crain, A. Curran, R. A. Campbell, C. A. Drubin, and W. F. Miccioli, "Millimeter-wave radar senor for automotive intelligent cruise control (ICC)" *microwave theory and techniques, IEEE Transactions on,* vol. 45 iss. 12 part: 2 , December 1997, pp. 2444-2453

[7]F. Kolak and C. Eswarappa, "A low profile 77 GHz three beam antenna for automotive radar" *microwave symposium, microwave theory and techniques, IEEE,* vol. 2, Digest 2001, pp. 1107-1110

[8]V. V. Denisenko, A. G. Shubov, A. V. Majorov, E. N. Egorov, and N. K. Kashaev, "Millimeter-wave printed circuit antenna system for automotive applications" *microwave symposium, microwave theory and techniques, IEEE,* vol. 3, May 2001, pp. 2247-2250

[9]D. M. Pozar, S. D. Targonski, and H. D. Syrigos, "Design of Millimeter Wave Microstrip Reflectarrays" *IEEE Transactions on Antennas And Propagation,* vol. 45, no. 2, February 1997, pp. 287-296

[10]R. D. Javor, X. D. Wu, and K. Chang, "Design and Performance of Microstrip Reflectarray Antenna" *IEEE Transactions on Antennas And Propagation,* vol. 43, no. 9, September 1995, pp. 932-939.

[11] J. Huang, "Microstrip Reflectarray," *in Proc. IEEE Int. Symp. Antennas Propagat,* on Canada, June 1991, pp. 612-615

[12]J. Huang, "Capabilities of Printed Reflectarray Antennas," I*EEE Phased Array Systems and Technology Symposium*, Boston, Massachusetts, October 1996, pp. 131-134

[13]J. Huang, "Bandwdith Study of Microstrip Reflectarray and A Novel Phased Reflectarray Concept," *in Proc. IEEE Trans. Antennas Propagat.*, vol. 45, February 1997, pp. 287-295

[14]K. Y. Sze, and L. Shafai, "Microstrip patches for a reflectarray" *IEEE international Symposium*, vol. 3, 1999, pp. 1666-1669

[15]D. G. Barry et al, "The Reflectarray Antenna, " *IEEE Trans, Antennas and Propagation,* vol. AP-11, Nov, 1963, pp. 645-651

[16]J. Huang, "The Development of Inflatable Array Antennas", *IEEE antennas and Propagation Magazine,* vol. 43, No. 4, August 2001, pp.44-50

[17]W. L. Stutzman and Gary A. Thiele, *Antenna Theory and Design.* New York: John Wiley & Sons, Inc. 1997.

[18]D. Pilz and W. Menzel, "Folded Reflectarray Antenna" *ELECTRONICS LETTERS 30th* vol. 34, no. 9, April 1998, pp. 832-833

[19]W. Menzel, D. Pilz, and R. Leberer, "A 77GHz FM/CW Radar Frontend with A Low-profile, Low-loss Printed Antenna" *IEEE MTT-S Digest,* pp. 1485-1488, 1999.

[20]R. D. Javor, Xiao-Dong Wu, and Kai Chang, "Beam Steering of A Microstrip Flat Reflectarray Antenna" *AP-S, Digest*, vol. 2, 1994, pp. 956-959

[21]R. D. Javor, X. D. Wu and K. Chang "Offset-fed Microstrip Reflectarray Antenna" *Electronic Letters 18th* vol. 30, no. 17 August 1994, pp.1363-1365

[22]V. G. Borkar, V. M. Pandharipande, and R. Ethiraj, "Millimeter Wave Twist Reflector Design Aspects" *IEEE Transactions on Antennas And Propagation,* vol. 40, no. 11, NOVEMBER 1992, pp.1423-1426

[23]D. M. Pozar, Microwave Engineering. New York: John Wiley & Sons, Inc. 1998